JOURNAL OF MATERIALS SCIENCE 33 (1998) 3479–3488

Ductility and toughenability study of epoxy resins under multiaxial stress states

H. KISHI*, Y.-B. SHI‡, J. HUANG, A. F. YEE§
Department of Materials Science and Engineering, University of Michigan, Dow Building, 2300 Hayward Street, Ann Arbor, MI 48109, USA
E-mail: afyee@umich.edu

The local strains in unmodified and rubber-modified epoxies under multiaxial stress states were examined. Matrix ductility was varied by using epoxide resins of different epoxide monomer molecular weights. The stress state was altered from a plane strain case to a plane stress case by varying the thickness of the test specimens. It was confirmed that, in the case of unmodified resins, the thinner specimens which experienced nearly uniaxial tensile stress exhibited much higher local strains at failure than the thicker counterparts which experienced highly triaxial tensile stress. Also, the cross-link density was reduced as monomer molecular weight increased, thus the increase in local plastic strain due to the stress state change also became greater. Furthermore, it was found that rubber modification markedly increased the plastic strain to failure, irrespective of the specimen dimensions, and that the extent of this plastic strain increased as cross-link density was lowered. These results are consistent with the concept that the cavitation of rubber particles relieves the initial multiaxial constraint in a thick specimen, induces a stress state closer to plane stress throughout the specimen, and consequently enables the matrix to deform to a larger extent. The results also show clearly that the toughenability of a matrix resin is not independent of the stress state and the matrix ductility.

1. Introduction

Thermosetting resins are used widely as structural materials and adhesives in the aerospace and electronics industries because of their high strength, high elastic modulus, and good heat and solvent resistance. It has been reasoned that these desirable properties originate from the resin's cross-linked structure [1]. However, an undesirable property is their low fracture toughness relative to thermoplastic resins, and they therefore need to be toughened if their range of applications is to be extended.

It is known that relatively low cross-link density epoxy resins can be toughened by the incorporation of elastomer particles, but more highly cross-linked epoxy resins are difficult to toughen in this way [2, 3]. McGarry *et al.* [4–6], Bascom *et al.* [7, 8] Pearson and Yee [2, 9, 10], Sue [11] and Kinloch *et al.* [3, 12, 13] have studied the toughening mechanisms in the elastomer-toughening technique. The current paper is not intended to be a comprehensive review on the subject of rubber toughening of epoxies, and hence only the work most relevant to our aims here is discussed below. McGarry *et al.* [4] and Bascom *et al.* [7] demonstrated the toughening effect of carboxyl-terminated butadiene-acrylonitrile (CTBN) rubber particles. The explanation of the mechanism at that early stage was mostly on a macroscopic level in that the crack tip plastic zone radius and the fracture toughness were the only parameters mentioned, and terms describing particle-size level and microscale mechanisms involving triaxial stress, constraint relief, hole growth, etc., were not discussed. Kinloch *et al.* [12] noted some of the essential characteristics of the mechanisms of rubber toughening in using caviation, dilation and shear to explain the observed toughening. However, a more exact mechanism, which is akin to the void formation and dilation as described in the metals literature, was not elucidated and a clear picture describing the exact particle-size level mechanism was not given. In more recent years, there has been some agreement that the mechanism of rubber toughening is very similar to that occurring in metals [14, 15]. Lazzeri and Bucknall [14, 15] hold the opinion that void formation and subsequent plastic void growth are the most fundamental mechanisms of rubber toughening. According to Yee and Pearson, the role of the elastomer particles is to relieve the constraint in front of the crack tip by cavitation [9, 10].

*Present address: Toray Industries, Inc., Composite Materials Research Laboratories, 1515, Tsutsui, Masaki-cho, Iyogun, Ehime 791–31, Japan.
‡Present address: Chrysler Corporation, Vehicle Crash Engineering, 800 Chrysler Drive East, Auburn Hills, MI 48326, USA.
§Author to whom all correspondence should be addressed.

This mechanism then alters the stress field from one dominated by triaxial stress, which causes brittle fracture, to one dominated by deviatoric stress [11], which promotes the formation of shear bands in the matrix resin [2, 9, 10]. Following this line of analysis, the change in the stress state is considered to be a trigger for the formation of shear bands. Additionally, the intrinsic ability of the matrix resin to deform plastically, i.e. its "ductility", is considered a vital requirement for the elastomer-toughening technique to be effective, and this intrinsic ability has been termed "toughenability" [2]. Therefore, the lower elastomer-toughenability of highly cross-linked networks could be a consequence of their low intrinsic ductility [2].

In general, the deformation behaviour of materials depends very much on the given stress state. Therefore, to be precise, the term "ductility" is meaningful only if the stress state is also specified. The term "ductility", traditionally used in the deformation study of metallic materials, has been used rather ambiguously in the field of polymers. In connection with this, the term "toughenability" [2] has also been used to refer to the ability of a polymer to be toughened. However, these concepts and their relationships have not been clearly defined due to the lack of understanding of the stress-state-dependent behaviour of polymers. In plane strain fracture toughness tests, the stress experienced by the material ahead of a crack tip is one of highly triaxial tension. Therefore, within the context of toughening, the deformation behaviour of polymers under dilatational (highly triaxial tensile) stress states should be carefully considered. Yee *et al.* [16] used the symmetric double-grooved strip tensile test to create biaxial tensile stress states and to examine the change in the apparent yield stress. They reasoned qualitatively that when the rubber concentration is sufficiently high, constraint relief caused by the rubber cavitation can change the stress state in modified epoxy specimens from the plane strain towards the plane stress state. In order to verify this idea more clearly, more quantitative studies on local deformation behaviour of polymers under both plane strain and plane stress states are necessary.

The objective of the present study was two-fold. First, to observe the local deformation behaviour under specific stress states and obtain measurement of the plastic strain. Second, based on results from rubber-toughened epoxies, to explain the dependence of deformation behaviour on stress state. We also examined the relationship between "ductility" and "toughenability" of the epoxy matrix.

2. Experimental procedure

2.1. Materials

Matrix ductility was altered by using epoxide resins of varying epoxide monomer molecular weights [2]. The epoxy resins used in this investigation were three kinds of diglycidyl ethers of bisphenol-A (DGEBA) based resin, designated as DER661®, DER664®, and DER667®, provided by the Dow Chemical Company. These resins are families of oligomers with the same basic chemical composition but different molecular weights. The average epoxy equivalent weight of each resin is 525, 925 and 1800 g/eq, respectively. Each resin was cured with the stoichiometric amount of 4,4′-diamino diphenyl sulphone (DDS), Sumicure-S®, provided by the Sumitomo Chemical Co. The active amino-hydrogen equivalent weight of DDS is 62 g/eq. The curing mechanism is predominantly by amine addition. Therefore, the resulting cross-link density (the molecular weight between cross-links) of a series of cured resins can be systematically controlled.

Pre-formed polyamide particles, designated as SP-500®, manufactured by Toray Industries, Inc., were mixed with the epoxy resins as deformation markers to examine the local strain of a series of cured neat resins. The particles consisted primarily of Nylon-12 and were spherical in shape with 6 μm average diameter. The amount of particles used was 0.5 wt %. It was supposed that the behaviour of the resin under study would not be significantly altered at such a low concentration, and indeed this assumption was verified as shown later.

Toughened epoxy resins were prepared by incorporating 10 vol % carboxyl-terminated butadiene-acrylonitrile liquid rubber, Hycar® CTBN 1300X13 supplied by the B.F. Goodrich Company, as the toughening modifier. Polyamide particles were also used as deformation markers in these CTBN-toughened systems and the amount of particles was again 0.5 wt %.

2.2. Fabrication of epoxy plaques

The epoxide equivalent weight of the resins used in this work ranged from 525–1800 g/eq., and this difference gave rise to a viscosity difference between resins. Therefore, two kinds of procedure were used for the preparation of the epoxy plaques, as shown in Table I. First, each resin composition without DDS was heated to the desired temperature in an oil bath and stirred to make a homogeneous mixture. Next, the stoichiometric amount of DDS was added to the resin mixture while stirring for 15 min, until the DDS was completely dissolved in the epoxy resin. This was followed by vacuum degassing for 10 min at the same temperature. Finally, the resin was cast into a pre-heated mould treated with a release agent. The resin was then cured in accordance with the schedule as shown in Table I. After curing, the oven was switched off and the cured resin was allowed to cool slowly to room temperature.

TABLE I Curing procedures for the preparation of epoxy plaques

Resin	Preheating cycle		Mixing/degassing cycle		Cure schedule		Post-cure schedule	
	(°C)	(h)	(°C)	(min)	(°C)	(h)	(°C)	(h)
DER661	140	> 1	140	~45	140	16	200	2
DER664	160	> 1	160	~20	160	16	200	2
DER667	160	> 1	160	~20	160	16	200	2

TABLE II Properties of the resins (cited from [2])

Formulation	G_e^a (dyn cm^{-2})	M_{nc} from G_e (g mol^{-1})	T_g (°C)	M_{nc} from T_g (g mol^{-1})	E (MPa)	G_{IC} (J m^{-2})	σ_y (MPa)
DER661/DDS	2.8×10^7	1160	120	1350	3360	201	96.1
DER664/DDS	2.0×10^7	1600	105	2800	–	–	–
DER667/DDS	7.0×10^6	4350	100	4300	3360	326	85.6
661/DDS/CTBN	–	–	–	–	3000	3000	81.5
664/DDS/CTBN	–	–	–	–	–	4500	–
667/DDS/CTBN	–	–	–	–	3000	11400	73.3

[a]The shear modulus of the rubbery plateau.

The resins, formulations, and curing schedules used in our study were exactly the same as those studied by Pearson and Yee [2]. Therefore, it was assumed that the molecular weight between cross-links, M_{nc}, and the physical and mechanical properties, such as glass transition temperature, T_g, and intrinsic ductility, of the cured resins were similar to those reported by Pearson and Yee [2]. The properties of the resins as measured by Pearson and Yee are cited in Table II for reference.

2.3. Symmetric double-notched plate tensile test

Multiaxial tensile stress states were created by using the symmetric double-notched plate tensile specimens, Fig. 1. Testing using such a specimen geometry gives rise to multiaxial tensile stress states as a result of stress concentration and geometric constraint. The stress state can be altered by changing the thickness of the specimens, defined in Fig. 1, which thus allows us to examine the deformation behaviour of the resins under various stress states. The symmetric double-notched plate tensile test as a means of multiaxial testing has been used in the field of metals research [17], but it has not been widely utilized in polymers research except for a preliminary attempt by Yee *et al.* [16, 18] and a blunt-notch variation used by Narisawa *et al.* [19] for crazing studies of thermoplastic polymers. Yee *et al.* [18] used the symmetric double-notched plate tensile samples to study brittle–ductile transitions of thermoplastic polymers by changing the specimen thickness as defined in the figure. Likewise, in this study, we make use of this specimen geometry to investigate the stress-state dependent deformation and failure behaviour of polymers, and the difference in the plastic strain of a series of cured resins under the same stress state.

In the symmetric double-notched tensile specimens, the round notches were machined with a diamond powder-coated grinding wheel to reduce the size of surface defects. The apparent gauge length, i.e. the height of the groove, h, was 3.2 mm, but it is not the true gauge length because the deformation at the notch root is not uniform. The ligament width between the two notches, w was 3.1 mm. The specimen width outside the notch section was 6.3 mm. Two thicknesses, T, were chosen to produce different multiaxial tensile stress states: one was 1 mm and the other was 7 mm. In the case of the thinner specimen, the

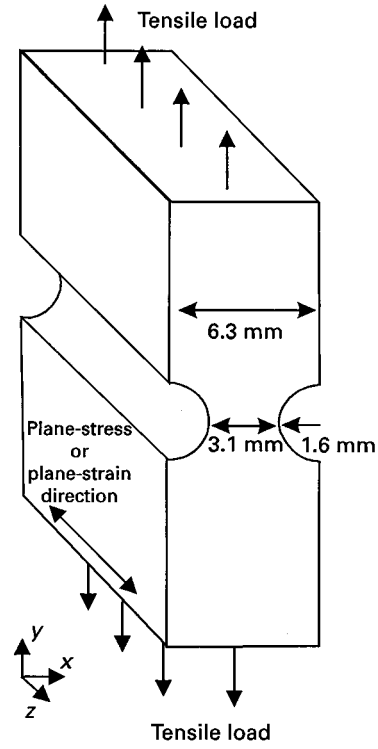

Figure 1 Illustration of a "symmetric double-notched plate tensile" specimen. The thickness direction is defined as the Z direction on the diagram.

stress state directly ahead of the notch tip must be nearly uniaxial, then the stress becomes increasingly biaxial at locations closer to the middle of the ligament of the specimen. On the other hand, in the thicker specimen, the stress state ahead of the notch always exhibits some triaxiality. In particular, the stress state in front of the slip-line field has been confirmed to possess a large triaxial component [20, 21].

A screw-driven Instron (Model 4502) was used to conduct the tensile tests. To ensure that yielding instead of brittle fracture occurred, a relatively slow crosshead speed (1 mm min^{-1}) was employed. The tensile tests were performed until failure of specimens or the critical point just before failure was reached.

2.4. Microscopy

Microscopy techniques were utilized to examine the deformation behaviour and to measure the plastic

strains. The subsurface deformation zones of the tested specimens were observed using an optical microscope (OM) "Nikon Optiphot" in the transmitted light mode, under both bright-field and cross-polarized light. Polished petrographic thin sections (25 μm thick), perpendicular to the fracture surface and encompassing the damage zone in front of the notch, were prepared for observation of deformation behaviour. Three regions were chosen to reveal the deformation behaviour under various stress states, as shown in Fig. 2. In the case of the thin specimens, Case A, the *yz*-plane view of the polished sections from immediately adjacent to the notch tip was examined. At this location, a nearly uniaxial tensile stress state exists because no constraint in the *x*-direction is created at the surface of a specimen and almost no stress in the *z*-direction exists in such a thin specimen. In the case of the thick specimens, Case B, the *xy*-plane view of the mid-plane in the thickness direction (*z*-direction) was examined. In pure epoxy cases where, under a plane-strain state, slip lines occurred in front of the blunt notch, the tip area of the slip-line field was examined closely for its high triaxiality. For CTBN-modified epoxies, in order to compare the degree of constraint, only thick specimens were used. Again the *xy*-plane view of the mid-plane in the thickness direction (*z*-direction) was examined, Case C. However, the location of observation was extended from near the notch tip to the middle of the ligament. The constraint should increase further from the notch tips.

2.5. Ductility assessment

The pre-formed polyamide particles dispersed in the epoxy resins could be used as deformation markers because they adhered to and deformed with the matrix without any interfacial failure. Furthermore, the Young's modulus of Nylon-12, 1100 MPa, is lower than that of the lowest T_g epoxy at the test temperature, while Poisson's ratio of most isotropic solid polymers lies between 0.35 and 0.42 [22]. So, the extent of plastic deformation experienced by the particle was considered virtually the same as the deformation of the surrounding matrix resin. Therefore, the ductility (the plastic strain) of the matrix resin under a given stress state could be assessed by determining the strain of the particles within a particular region of the damage zone as captured by microscopy. The following three assumptions were made in calculating the plastic strain of the particles:

1. the volume of a particle is constant during the plastic deformation process;
2. the deformation throughout a particle is uniform;
3. the cut plane is parallel to the loading direction.

The first assumption is often used for the plastic deformation process and is reasonable because plastic deformation is a shearing process and so does not involve dilatation. If the second assumption is valid, then the shape of a particle becomes perfectly elliptical after deformation. In our study, this assumption was experimentally verified by comparing the magnified images of actual particles with shapes of true ellipses.

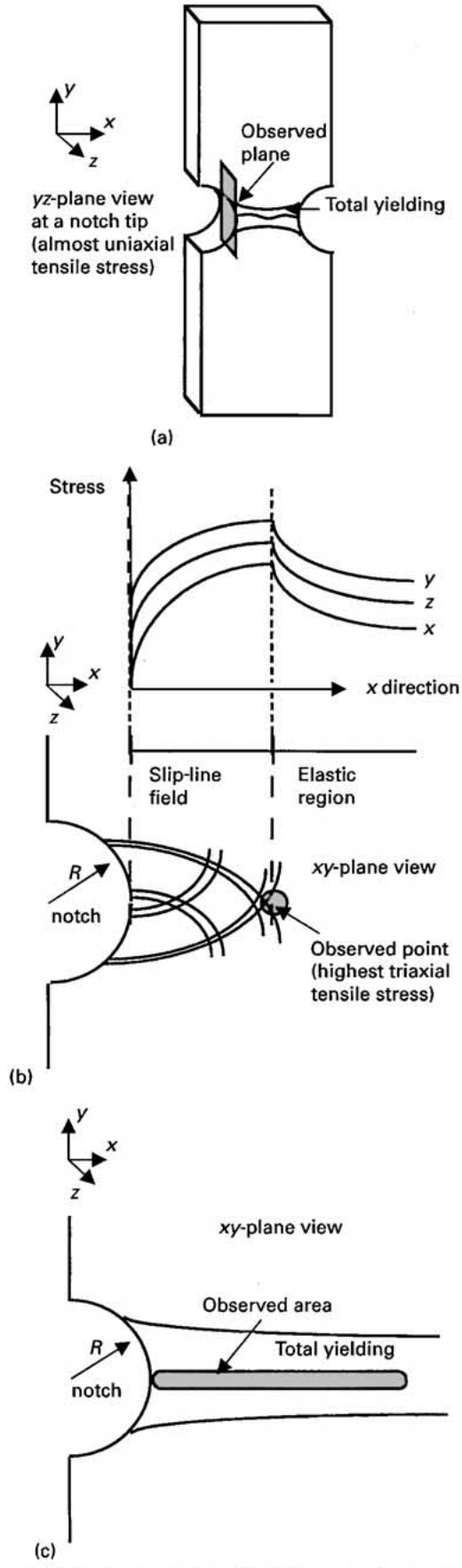

Figure 2 Illustration of regions observed on the deformation behaviour under various stress states (a) Case A: *yz*-plane view directly next to a notch tip, in thin specimens of pure epoxies. (b) Case B: *xy*-plane view of the mid-plane in the thickness direction, in thick specimens of pure epoxies. Attention was focused on the tip area of the slip-line field. (c) Case C: *xy*-plane view of a strip of the mid-plane in the thickness direction, in thick specimens of CTBN-modified epoxies. The observed location is extended from near the notch tip to the middle of the ligament.

The third assumption is applicable to perfect ellipsoids. The aspect ratio of an ellipsoid remains the same regardless of the cutting point so long as the cut plane is parallel to the loading direction. Therefore, although the observed plane does not necessarily cut through the centre of each particle, the aspect ratio is still good for strain calculation. Now, let us imagine a virtual ellipsoid which has a centre plane on the observed plane as captured by microscopy. From the third assumption, the virtual ellipsoid has the same strain as the actual particle. The volume of the deformed virtual particle, V_p and the volume of the pre-deformed virtual spherical particle, V_o, were calculated from Equations 1 and 2, respectively

$$V_p = 4\pi ab^2/3 \quad (1)$$

$$V_o = 4\pi r_o^3/3 \quad (2)$$

where a is half of the major axis of the deformed particle, b is half of the minor axis of the deformed particle, and r_o is the radius of the pre-deformed virtual particle. From the first assumption, V_p equals V_o. Then r_o could be calculated from Equation 3

$$r_o = (ab^2)^{1/3} \quad (3)$$

The plastic strain, ε, of a particle was then calculated by using Equation 4

$$\varepsilon = (a/b)^{2/3} - 1 \quad (4)$$

Although this method of determining plastic strains may not be subject to a particularly high degree of accuracy, it is considered to be sufficient for comparing the effects of M_{nc} and rubber modification on ductility.

3. Results and discussion

3.1. Deformation behaviour of pure epoxies under uniaxial tension and triaxial tension

When specimens were thin enough, total yielding occurred and shrinkage in the thickness direction (z-direction) was observed in all three kinds of epoxy resin. The yz-plane view of a notch tip of pure epoxy resins after failure was examined under OM in bright-field. Fig. 3 includes micrographs of (a) DER661/DDS and (b) DER667/DDS. Under the microscope, intersecting type shear bands were observed in the yielded zone in the yz-plane, which is the characteristic of plane-stress deformation [23]. This is consistent with the stress state at the notch tip being close to uniaxial tension. Fig. 4 shows micrographs of polyamide particles taken at a higher magnification from the centre area of the intersecting type shear bands. As a reference, particles before loading are shown in Fig. 5. Both large deformation of particles, and good adhesion between particles and the matrix resins can be observed in Fig. 4. Therefore, the extent of deformation of the particles must follow the deformation of the surrounding matrix resin. Our observation of the extent of elongation of the particles indicates that the matrix deformation increased with increasing M_{nc} of the matrix resin.

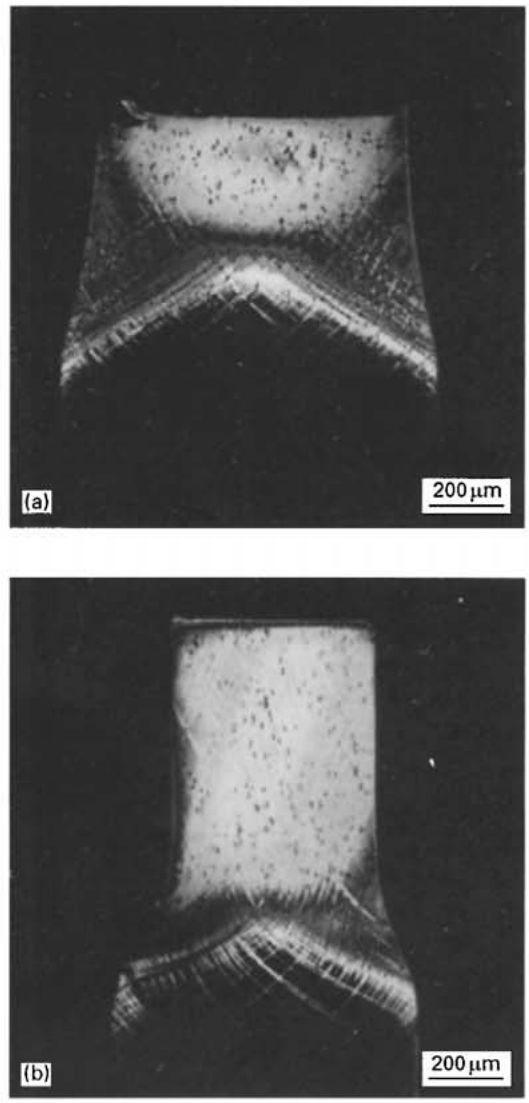

Figure 3 Optical micrograph, in the yz-plane view, of a polished section taken from immediately adjacent to a notch tip. (a) Thin specimen of DER661/DDS, including 0.5 wt % Nylon-12 particles as deformation markers. (b) Thin specimen of DER667/DDS, including 0.5 wt % Nylon-12 particles as deformation markers.

Fig. 6 shows the deformation zones of the thick specimens of (a) DER661/DDS and (b) DER667/DDS. These specimens were loaded to the critical point just before failure. The xy-plane view of the area in front of a notch was examined. In this case, a plane-strain condition, slip-line type shear deformation occurred. The size of the slip-line field of DER667/DDS was almost identical to that of DER661/DDS, despite the difference in their M_{nc}. This suggests that under highly triaxial tension the lower cross-link density epoxy responds in a similar way to the higher cross-link density epoxy, which may partly explain the small effect of M_{nc} on the fracture toughness, as reported previously [2]. The plastic–elastic boundary, i.e. the tip of the slip-line field, of the two materials is shown magnified in Fig. 7. Regardless of the M_{nc} of the matrix resin, the spherical shape of the particles was maintained. This clearly indicates that at the plastic–elastic boundary, the stress state must be highly triaxial. This also demonstrates that, with no apparent plastic deformation observed, the hydrostatic stress

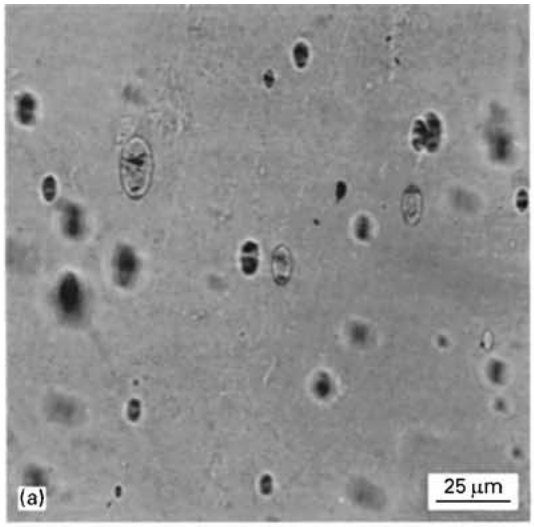

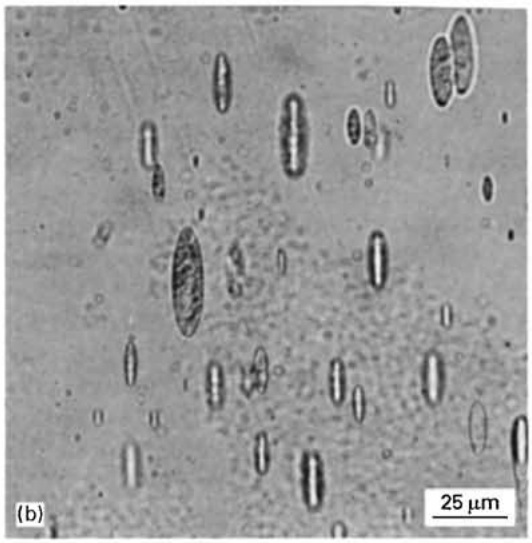

Figure 4 As Fig. 3 but at a higher magnification. Note that the deformation of the particles in DER667/DDS (b), is larger than that in DER661/DDS (a).

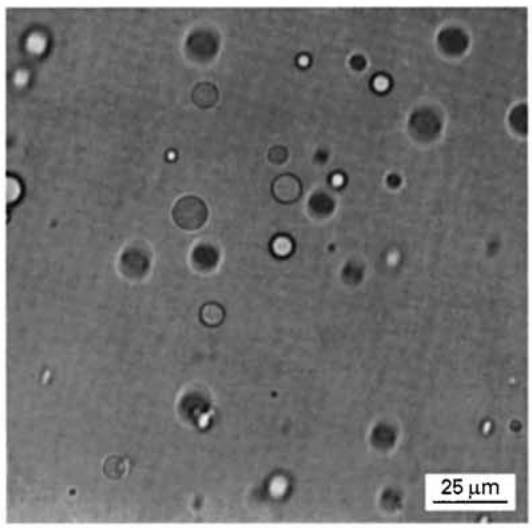

Figure 5 Nylon-12 particles embedded in an unloaded DER667/DDS specimen. Note that the particles are not deformed and maintain the spherical shape.

component dominates in this highly triaxial tension stress state. Again it can be seen that, under highly triaxial tension, the lower cross-link density epoxy

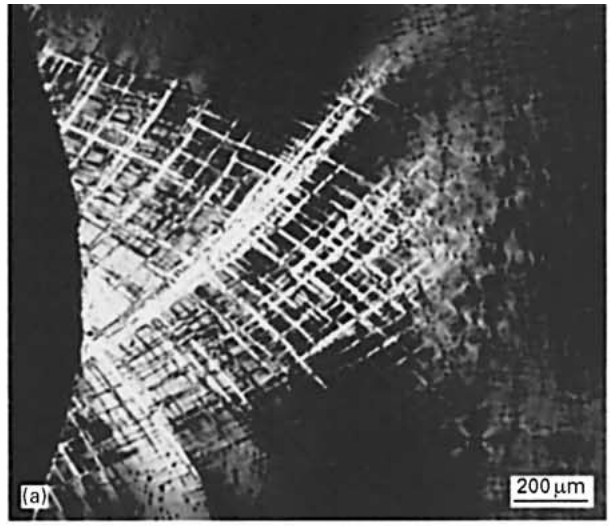

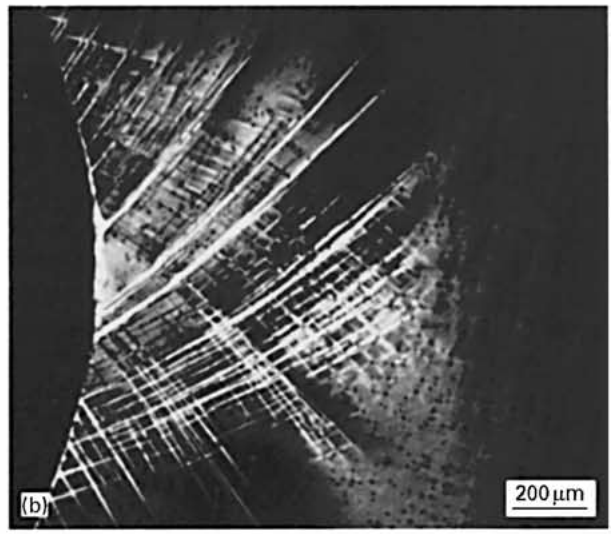

Figure 6 Optical micrograph, in xy-plane view, of a polished section taken from the mid-plane in the thickness direction. (a) Thick specimen of DER661/DDS, including 0.5 wt % Nylon-12 particles as deformation markers, loaded to the critical point just before failure. (b) Thick specimen of DER667/DDS, including 0.5 wt % Nylon-12 particles as deformation markers, loaded to the critical point just before failure.

responds in a similar way to the higher cross-link density epoxy. Another interesting phenomenon observed was that "craze-like" microcracks appeared in some particles in the tip region of the slip-line field. No such microcracks were observed in particles located closer to the notch tip. This observation indicates that the tip of the slip-line field has higher triaxiality than the notch tip area, because the void formation required for crazing involves a dilatational process [19,24].

So far, only a qualitative explanation of the deformation behaviour of the pure epoxies has been provided. Our objective was, however, to determine the plastic strain quantitatively. Fig. 8 shows a high-magnification image of a polyamide particle which was taken from a failed thin specimen of DER667/DDS. We verified that the particle shape was almost truly elliptical by comparing it with a true ellipse generated using a computer. The same experimental verification of the shape of the particles was performed for more

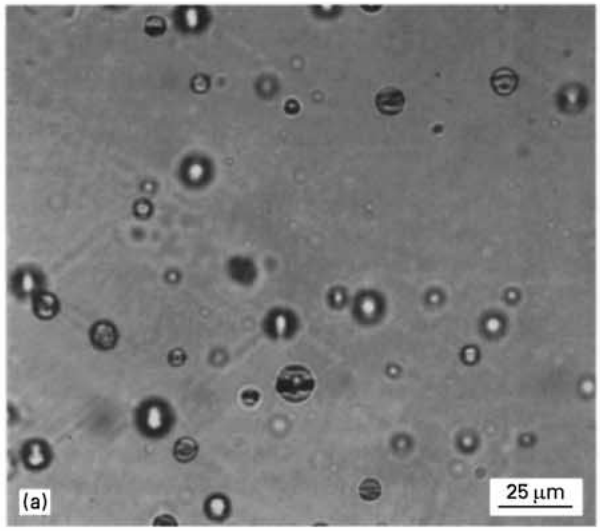

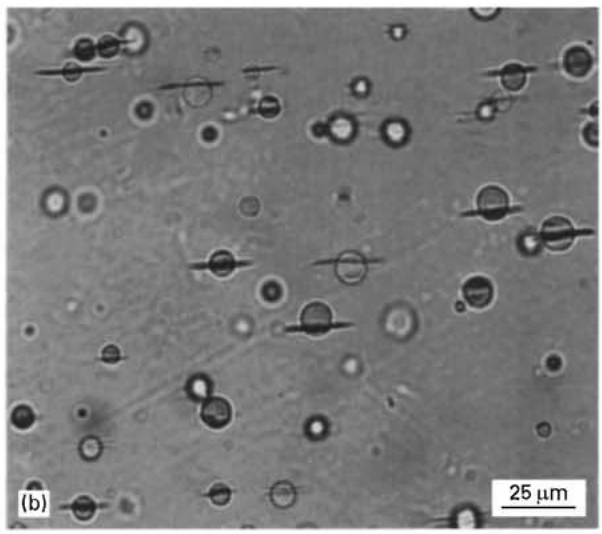

Figure 7 As Fig. 6 but showing the tip of the slip-line field at a higher magnification. Note that the spherical shape of the particles is maintained, regardless of the difference in their M_{nc} of the matrix resin.

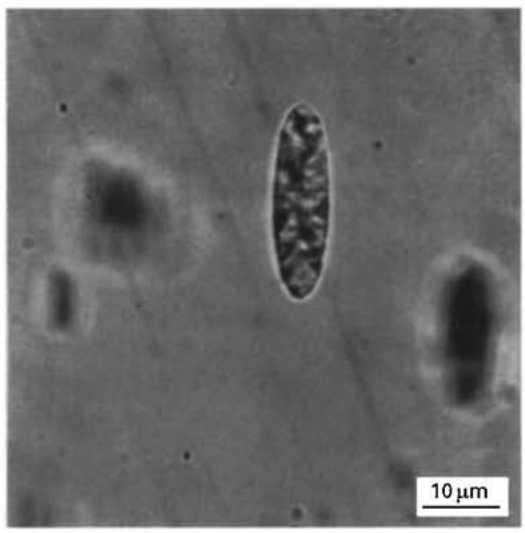

Figure 8 Optical micrograph of a high-magnification image of Nylon-12 particles which are embedded in a failed thin specimen of DER667/DDS.

than five particles from each resin. The existence of perfect elliptical shapes implies that the particles and the surrounding matrix resin in the observed areas

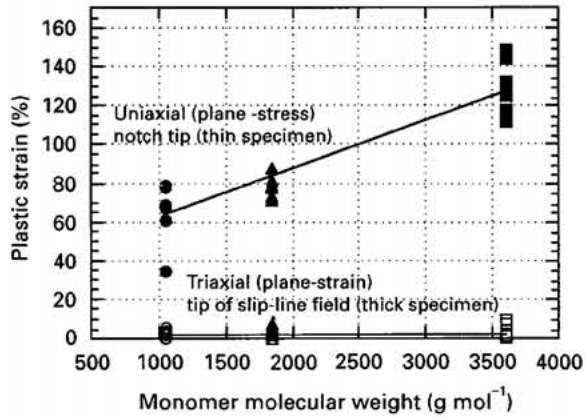

Figure 9 The effect of stress state on the plastic strain of pure epoxies with various cross-link densities. Note that the strain under high triaxial tension did not increase with decreasing cross-link density. On the other hand, the plastic strain under uniaxial tension increased markedly with decreasing cross-link density.

experienced practically uniform deformation. By measuring the lengths of the major axis and the minor axis of each particle, the plastic strain of the particle could be calculated from Equations 1–4. As explained in Section 2, it is presumed that the strain of the particles reflects the strain of the surrounding matrix. Fig. 9 shows the relationship between the calculated plastic strain and the epoxy monomer molecular weight. The higher the monomer molecular weight, the lower the cross-link density of the resin. The plastic strains of each resin under both uniaxial tension and highly triaxial tension are plotted on the figure. The thin specimens, which failed under uniaxial tension (plane-stress state), exhibited much higher plastic strain than the thick specimens, which failed under highly triaxial tension (plane-strain state). The strain under highly triaxial tension did not increase with decreasing cross-link density. On the other hand, the plastic strain under uniaxial tension increased markedly with decreasing cross-link density. This trend of plastic strain versus cross-link density is similar to the trend in the rubber-toughening effect versus cross-link density as observed by Pearson and Yee [2], whose results are shown in Fig. 10.

3.2. Deformation behaviour of thick specimens of CTBN-modified epoxies

Fig. 11 shows the deformation zones of the thick specimens of the CTBN-modified DER661/DDS (a,b) and the CTBN-modified DER667/DDS (c,d). Again these specimens were loaded to the critical point just before failure. The xy-plane view of the notch tip area was observed. Compared with the slip-line type shear deformation of the pure epoxies, the slip lines of the CTBN-modified epoxies were diffuse. The shear lines eventually connected the two notches of a specimen and total yielding of the necked region occurred. The size of the slip-line field of the CTBN-modified DER667/DDS was larger than that of the CTBN-modified DER661/DDS; this was different from the cases of non-modified epoxies. This observation suggests

that the lower cross-link density CTBN-modified epoxy can deform to a larger extent than the higher cross-link density modified epoxy, even within a geometry that experiences high initial triaxial tension. One important point in these thick specimens is that almost all rubber particles in the observed region were cavitated after loading (Fig. 12). If local constraint relief is induced by the rubber cavitation and this relief can change the local stress state from a plane-strain state towards a plane-stress one, as proposed by Yee *et al.* [16], then this change in stress state should be reflected in the extent of strain. So the macroscopic change of deformation behaviour due to rubber-modification apparently suggests that a microscopic stress state change might have occurred in the thick specimens (which originally would have sustained highly triaxial tension in front of a notch). A plausible sequence of events under loading is as follows: (1) initial slip-line type plastic deformation occurs in front of the blunt notches due to stress concentration; (2) at the tip of the slip-line field, triaxial tension arises due to the plastic constraint; (3) rubber cavitation occurs when the triaxial tension reaches a critical value; (4) the cavitation causes some amount of constraint relief locally; (5) if the constraint relief is sufficient, the local stress state can change from plane strain towards plane stress; (6) this stress state change causes the deformation to switch from being microscopically non-uniform (localized) mode to being more uniform. Therefore, slip lines (i.e. localized deformation) become diffused and less distinguishable.

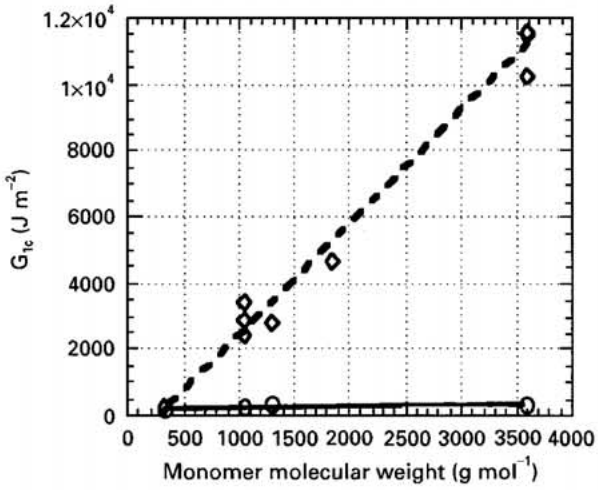

Figure 10 The relationship between toughness and cross-link density of pure epoxies, (E), and CTBN-modified epoxies (A), cited from a paper published by Pearson and Yee [2]. The trend of rubber-toughening effect versus cross-link density is similar to the trend in plastic strain under uniaxial tensile stress on cross-link density. By contrast, the toughness of pure epoxies has no dependence on the cross-link density similar to the trend in strain under triaxial tension, shown in Fig.9.

Fig. 13 shows high-magnification images of polyamide particles taken from the failed thick specimens of (a) CTBN-modified DER661/DDS and (b) CTBN-modified DER667/DDS. The polyamide particles in the CTBN-modified epoxies were elongated in spite of being embedded in thick specimens. The particles in

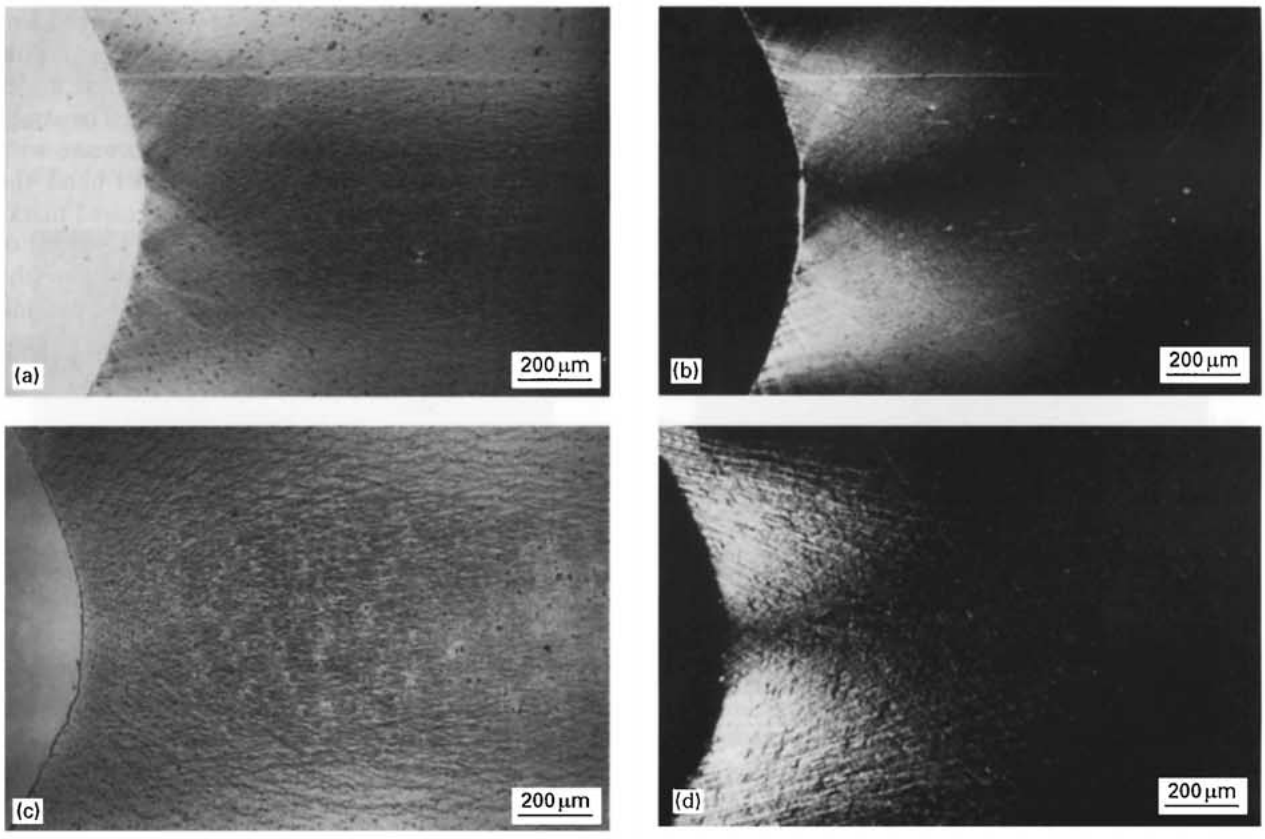

Figure 11 Optical micrograph, in *xy*-plane view, of a polished section taken from the mid-plane in the thickness direction, viewed in (a,c) bright-field and (b,d) cross-polarized light. (a,b) Thick specimen of CTBN-modified DER661/DDS, including 0.5 wt % Nylon-12 particles as deformation markers, loaded to the critical point just before failure. (c,d) Thick specimen of CTBN-modified DER667/DDS, including 0.5 wt % Nylon-12 particles as deformation markers, loaded to the critical point just before failure.

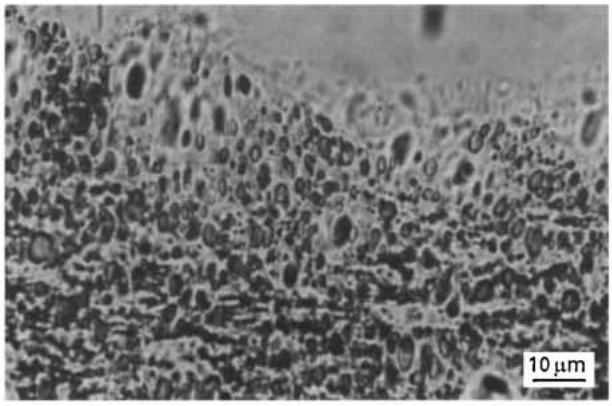

Figure 12 Optical micrograph, in *xy*-plane view, of the region below the fracture surface of a CTBN-modified DER667/DDS specimen. Note that almost all rubber particles were found to be cavitated after loading.

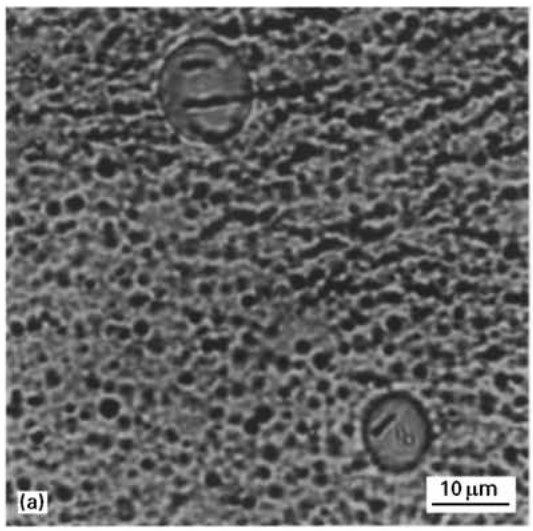

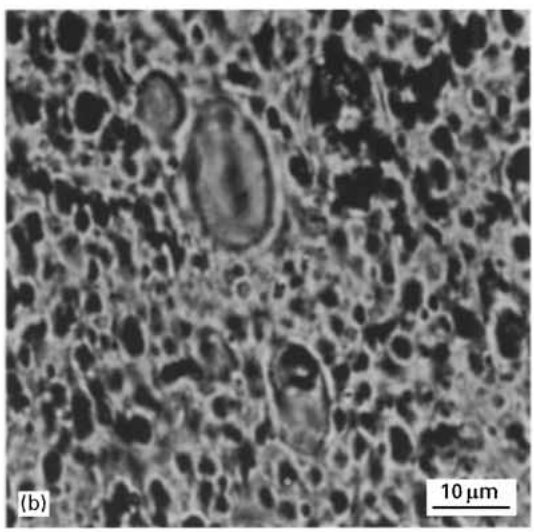

Figure 13 Optical micrograph of a high-magnification image of Nylon-12 particles which are embedded in a failed thick specimen of (a) CTBN-modified DER661/DDS and (b) CTBN-modified DER667/DDS. Note that the particles in the CTBN-modified epoxies are elongated in spite of being embedded in thick specimens. The particles in the lower cross-link density epoxy (b), showed higher strains than those in the high cross-link density epoxy (a).

the lower cross-link density epoxy showed higher strains than those in the higher cross-link density epoxy. Owing to the presence of the numerous smaller rubber particles, the boundary of a polyamide particle was not well defined in some cases. Because of the apparent roughness in the boundaries of the polyamide particles, strain calculations of the CTBN-modified epoxies have lower degrees of accuracy than in the corresponding unmodified epoxies, although they are still considered to be sufficient for comparing the effects of M_{nc} and rubber-modification on the plastic strain.

Based on the same calculation method as in the cases of the pure epoxies, the plastic strain in three CTBN-modified epoxies was characterized. For these CTBN-modified epoxies, observations were made from near the notch tip to the middle of the ligament. This was necessary because the slip-line field became diffused and it was therefore more difficult to pinpoint a location representing a certain stress-state. However, it is wholly reasonable that the constraint should become higher with increasing distance from the notch. Fig. 14 shows the relationship between the plastic strain and the distance from a notch. An overall observation is that rubber-modification markedly increased the plastic strain even in the thick specimens. Secondly, the location has a strong influence on the extent of the plastic strain observed. This second observation is probably due to the constraint level variation with location within a specimen. As a unit cell of material moves further away from a notch, the constraint increases and the plastic strain decreases. So, some constraint still exists in these rubber-modified specimens at the concentration of rubber toughener investigated. However, if the concentration of the rubber particles becomes sufficiently high, the constraint relief should effectively turn the stress state into one of purely plane-stress. In that event, the effect of location would no longer be significant.

In order to examine the relationship between the plastic strain and the cross-link density of matrix resins, the same data in Fig. 14 were replotted in Fig. 15. It can be seen that the extent of plastic strain increases with the decrease in cross-link density. It is

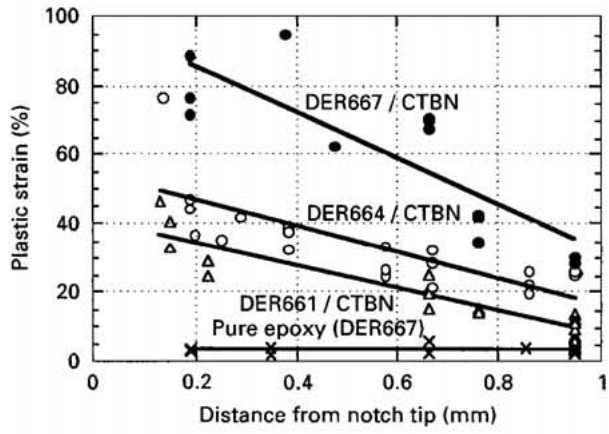

Figure 14 Relationship between the plastic strain and the distance from a notch of CTBN-modified epoxies.

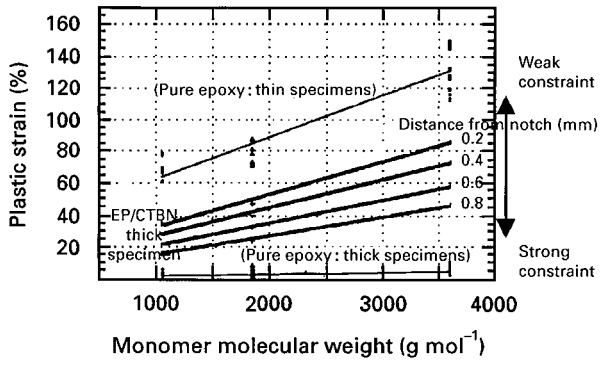

Figure 15 Relationship between the plastic strain and the cross-link density of CTBN-modified epoxies (thick specimens) and pure epoxies (both thin and thick specimens), derived from data in Figs. 14 and 9.

clear that the effect of rubber cavitation on the plastic strain increase is similar to that of decreasing the thickness in the pure epoxies, and is most probably due to constraint relief caused by rubber cavitation in the thick specimens. As mentioned earlier, the dependence of the plastic strain on cross-link density is similar to that of the matrix toughenability. In this study, constraint relief due to rubber cavitation was reasoned to cause a stress state change towards plane-stress. Our results also show that, under the plane-stress state, the lower cross-linked resin can undergo more plastic strain. This increased plastic strain is most likely to be responsible for the increase in energy absorbed, and thus the higher toughness [25]. It therefore seems reasonable to postulate that a strong relationship exists between the plastic deformation capability, i.e. "ductility", under plane-stress state and the ability to be toughened, i.e. "toughenability", of the matrix resin. However, the causal relationship between the "ductility" and the "toughenability" has not been fully quantitatively verified, because the measured value in the present study was the plastic strain, instead of the absorbed energy. To correlate the ultimate plastic strain of matrix resin with the crack initiation toughness increase induced by rubber-modification, various quantities must also be known including the size of the process zone in front of a crack tip, the stress and strain distribution within the process zone, and the stress–strain relationship of the matrix resin. Efforts in these areas are currently being made.

4. Conclusions

The deformation behaviour of materials depends very strongly on the stress state. Therefore, the term "ductility" is meaningful only where the stress state is also specified. In the present study, the local deformation behaviour of epoxies under both uniaxial and highly triaxial tension were observed, and the plastic strain was determined quantitatively. Based on these results, four conclusions could be drawn.

1. The stress state influences the extent of strain at failure.
2. Cross-link density – an intrinsic material property – dictates the achievable ductility.
3. Cavitation of rubber particles relieves the initial multiaxial constraint in a thick specimen, induces a stress state closer to plane stress, and consequently enables the matrix to deform to a larger extent.
4. The toughenability of a matrix resin is intimately related to the stress state and the matrix ductility.

Acknowledgements

This work was supported by a grant from the National Science Foundation, CMS-9523078. H. Kishi was supported by Toray Industries, Inc. We thank Drs Kazunao Kubotera and Jason Harcup, and Mr Jianguang Du for their useful input.

References

1. R. J. YOUNG and P. A. LOVELL, "Introduction to Polymers", 2nd Edn (Chapman and Hall, London, 1991) p. 4.
2. R. A. PEARSON and A. F. YEE, *J. Mater. Sci.* **24** (1989) 2571.
3. A. J. KINLOCH, C. A. FINCH and S. HASHEMI, *Polymer Commun.* **28** (1987) 322.
4. F. J. McGARRY, *Proc. R. Soc. Lond.* **A319** (1970) 59.
5. J. N. SULTAN, R. C. LAIBLE and F. J. McGARRY, *Appl. Polym. Symp.* **16** (1971) 127.
6. J. N. SULTAN and F. J. McGARRY, *Polym. Eng. Sci.* **13** (1973) 29.
7. W. D. BASCOM, R. L. COTTINGHAM, R. L. JONES and P. PEYSER, *J. Appl. Polym. Sci.* **19** (1975) 2545.
8. W. D. BASCOM, R. Y. TING, R. J. MOULTON, C. K. RIEW and A. R. SIEBERT, *J. Mater. Sci.* **16** (1981) 2657.
9. A. F. YEE and R. A. PEARSON, *J. Mater. Sci.* **21** (1986) 2462.
10. R. A. PEARSON and A. F. YEE, *ibid.* **21** (1986) 2475.
11. H.-J. SUE, PhD thesis, The University of Michigan, Ann Arbor, MI (1988).
12. A. J. KINLOCH, S. J. SHAW, D. A. TOD and D. L. HUNSTON, *Polymer* **24** (1983) 1341.
13. A. J. KINLOCH, in "Rubber-Toughened Plastics", *Advances in Chemistry Series* No. 222, edited by C. K. Riew (American Chemical Society, 1989) p. 67.
14. A. LAZZERI and C. B. BUCKNALL, *J. Mater. Sci.* **28** (1993) 6799.
15.. *Idem., Polymer* **36** (1995) 2895.
16. A. F. YEE, DONGMING LI and XIAOWEI LI, *J. Mater. Sci.* **28** (1993) 6392.
17. J. W. HANCOCK and D. K. BROWN, *J. Mech. Phys. Solids.* **31** (1) (1983) 1.
18. A. F. YEE, W. V. OLSZEWSKI and S. MILLER, in Advances in Chemistry Series No. 154, edited by R. D. Deanin and A. M. Crugnola (American Chemical Society, 1976) p. 97.
19. I. NARISAWA, M. ISHIKAWA and H. OGAWA, *J. Mater. Sci.* **15** (1980) 2059.
20. R. HILL, in "The Mathematical Theory of Plasticity" (Oxford University Press, 1950).
21. M. ISHIKAWA, I. NARISAWA and H. OGAWA, *J. Polym. Sci.* **15** (1977) 1791.
22. N. G. McCRUM, C. P. BUCKLEY and C. B. BUCKNALL, in "Principles of Polymer Engineering" (Oxford University Press, 1988) p. 347.
23. G. T. HAHN and A. R. ROSENFIELD, *Acta Metall.* **13** (1965) 293.
24. N. J. MILLS, *J. Mater. Sci.* **11** (1976) 363.
25. DONGMING Li, PhD thesis, The University of Michigan, Ann Arbor, MI (1993).

Received 23 February 1996
and accepted 22 April 1998